

Groundwater Dynamics and Salinity in Coastal Barriers

Peter Nielsen

Department of Civil Engineering
The University of Queensland
Brisbane, Australia 4072
email: P.Nielsen@mailbox.uq.edu.au

ABSTRACT

NIELSEN, P., 1999. Groundwater Dynamics and Salinity in Coastal Barriers. *Journal of Coastal Research*, 15(3), 732-740. Royal Palm Beach (Florida), ISSN 0749-0208.



A qualitative description based on field measurements is given together with a simple modelling framework for watertable heights and salinity structure in coastal barriers. In coastal barriers of width less than one kilometre the shape of the watertable and the salinity structure are quite different from the classical scenarios. On this scale the extra watertable height caused by wave runup on the ocean side can drive a significant landward ground water velocity. A primary consequence of this is that any wastewater released into the aquifer, including oil spills on the beach, will travel towards the land rather than towards the ocean. Secondly, this landward flow of salty groundwater makes the freshwater lens much thinner than the "Ghyben-Herzberg thickness". A shallow aquifer model is presented for the watertable including quantitative boundary conditions that account for the effects of waves and tides. The salinity structure is modelled in terms of the thickness of the freshwater lens, accounting for freshwater recharge as well as convective and diffusive salt transport. The field measurements indicate that 1D modelling can be done with a simple uncoupled model except within a narrow (one or two metres) diffusive boundary layer on the landward side of the barrier within which the freshwater displacement thickness varies very rapidly.

ADDITIONAL INDEX WORDS: *Salinity, coastal pollution, water table, ground water, wave setup, wave runup, tides, coastal barriers, atolls.*

INTRODUCTION

It has been known for some time that the action of waves and tides on sandy beaches tend to raise the coastal groundwater levels. With large waves and/or large tides on a flat slope, the overheight may be several metres. This means that the ground water dynamics in coastal barriers are often as shown in Figure 1.

The effect will be greater the more the landward side is protected from the waves and the tides. Also, if the landward side is steeper than the ocean side, the tidal superelevation is further reduced. These details will be discussed further in Sections 3 and 4. For a given difference in levels from the exposed to the protected side it is also clear that the watertable slope and hence the landward groundwater flow will be greater the narrower the barrier is.

The general picture of the groundwater flow shown in Figure 1 has a number of significant consequences for the environmental management of coastal barriers. Firstly, it must be noted that, contrary to what might have been expected, any wastewater released into the aquifer will travel towards the continent rather than towards the ocean. Secondly, the fact that there is a net inflow of water through the beach face means that pollutants that land on the beach face will have a strong tendency to enter the aquifer under the barrier. This means that the use of detergents to disperse oily pollutants from barrier beaches must be discouraged since it will, more

than anything, make the pollutants enter the barrier groundwater system with increased speed. Thirdly, the freshwater lens under such a barrier is thinner than in the classical Ghyben-Herzberg scenario and the vegetation may be subject to salt poisoning under extreme conditions of large waves after a period with low rainfall.

The nature of the processes and the probable ranges of conditions will be discussed in the following sections. Section 2 offers an introduction to the details of the coastal boundary condition for the groundwater system. Section 3 then considers the wave forcing both qualitatively and quantitatively. The effects of the tide are addressed in Section 4. The width of the coastal strip in which the effects of waves and tides are important for groundwater modelling is quantified in Section 5. The resulting groundwater dynamics in the interior are described in Section 6. Some dynamic aspects of the salinity structure are analysed in Section 7 and the likely residence times of pollutants are discussed.

THE COASTAL BOUNDARY

The watertable a few tens of metres inland from the high water mark on a beach will be considerably higher than the Mean Sea level (MSL) even if there is no outflow due to rainfall on the land. This overheight is partly due to waves and partly due to tides. The situation is illustrated in Figure 2 and a few useful definitions will be given below.

The long term average level of the ocean surface outside the surf zone is the mean sea level, MSL. The still water surface, SWS is the flat (on the scale considered) sea surface

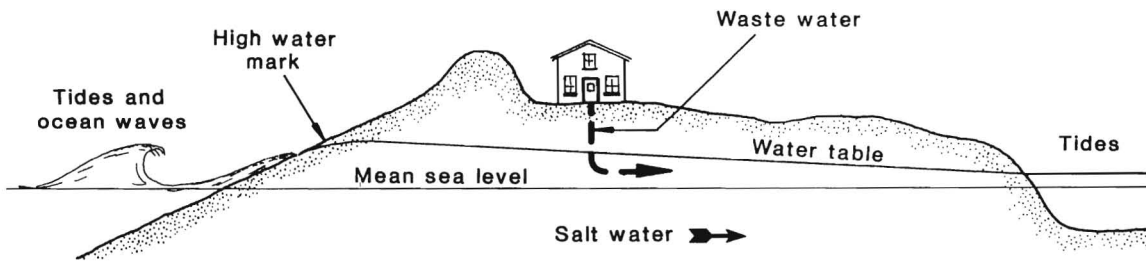


Figure 1. The watertable under coastal barriers will be highest near the ocean beach because of the action of waves and tides. Consequently there is a net flow of groundwater towards the continent and the fresh water lens tends to be very thin.

which would exist in the absence of winds and waves. It moves up and down due to astronomical tides and changes in barometric pressure. Local short time (15 to 20 minutes) averaging of the water level defines the mean water surface, MWS, which intersects the beach at the shoreline (SL) and becomes the watertable. The mean water surface/watertable is not a flat surface. Offshore of the breakpoint it may be a few centimetres below SWS due to wave setdown and inside the surf zone it rises towards the beach due to wave setup and wind setup. The watertable rises further landward of the shoreline. On a low tide, this rise may be caused partly by stored water from the previous high tide. On a rising tide, however, it is entirely due to the infiltration from wave run-up. This gives rise to the humped shape of the watertable with the hump being near the runup limit, RL. Landward of the high water mark (the high tide runup limit) the watertable oscillates inside an envelope (UENV, LENV) which tapers off to define an average superelevation η^+ above the mean sea level.

The landward range of the different oscillations depends on their period. Wind waves, surf beats and even tides are not felt more than a few tens of metres landward of the high water mark but oscillations due to wave height changes over several days reach further. See the data of NIELSEN *et al.* (1988), NIELSEN (1990) and KANG *et al.* (1994). The time averaged effects influence the boundary condition for regional groundwater modelling.

The fact that salty sea water is poured in on top throughout the swash zone means that the classical large scale scenario shown, *e.g.*, by COOPER (1959)—his Figure 5, must be supplemented with an area of sea water salinity on top of fresher water in the swash zone. For a tide free situation, the general flow pattern which is driven by the waves on the scale of the surf zone was illustrated and modelled by LONGUET-HIGGINS (1983).

The nature of the tidal watertable fluctuations on the two sides of a coastal barrier are shown in Figure 3.

Both gauges were of the order 10m inland of the respective high water marks. The watertable variation on the ocean side is largest when the waves are big because the wave setup brings "the action" closer to the well. The shape of the tidal signal is skewed towards a saw tooth shape, and the difference in watertable height between the wells is seen to correlate with the offshore wave height.

WAVE FORCING

As indicated by Figure 3, the contribution to the watertable height by wind waves varies on the time scale of hours as the height, H , period, T and direction of the off shore waves changes. The hydraulic conductivity, K of the sand and the changing beach topography will also play a role.

The amount of data is sparse and when extrapolating, it should be kept in mind that the inner surf-zone/swash-zone

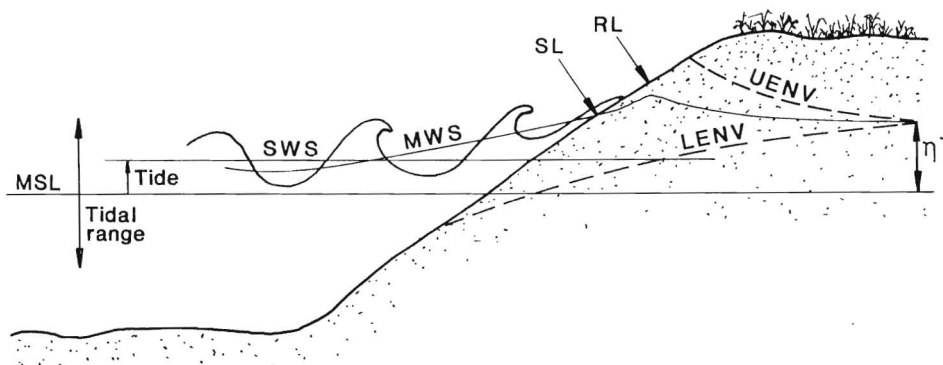


Figure 2. Definition sketch for terms used in formulating the coastal boundary condition for groundwater modelling.

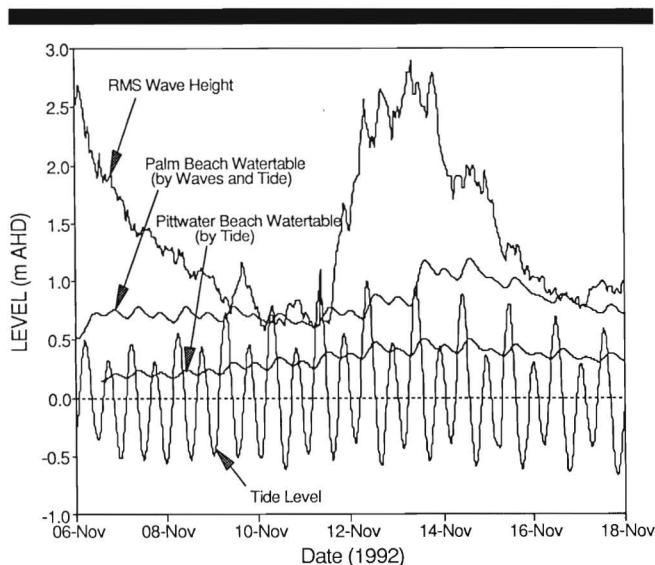


Figure 3. Watertable time series from the exposed (Palm Beach) and the protected (Pittwater) sides of the Palm Beach Isthmus, Sydney, Australia. The palm Beach Isthmus is approximately 200m wide at the site. The depth of sand to bed rock is of the order 25 metres, but organic layers of low permeability may exist close to MSL. Data courtesy of the New South Wales Department of Soil and Water Conservation.

hydrodynamics are very different on dissipative and reflective beaches. Reflective beaches (long waves on steep beaches) tend to have very vigorous windwave swash, see *e.g.* the photo of NIELSEN (1992) p 262 while dissipative beaches (steep waves on flat beaches) have little windwave swash but extensive waterline movements due to surf beat.

Regular Waves

Some of the above mentioned variables may be eliminated by considering laboratory experiments with regular waves like those of KANG (1995) which were also reported in some detail by KANG and NIELSEN (1994).

KANG found from experiments with two sand sizes (0.18mm and 0.78mm) that the ratio between the wave generated groundwater overheight and the runup height was independent of grain size and hence of the hydraulic conductivity

$$\eta_w^+/R \approx 0.62 \quad (1)$$

which with the formula

$$R = \sqrt{HL_o} \tan \beta_F \quad (2)$$

for the runup height (*cf.* NIELSEN and HANSLOW 1991) leads to

$$\eta_w^+ \approx 0.62 \sqrt{HL_o} \tan \beta_F \quad (3)$$

where H is the wave height in the uniform part of the flume, the deep water wave length is calculated from linear wave theory:

$$L_o = gT^2/2\pi \quad (4)$$

and β_F is the slope of the beach face. Some details of the

underlying distribution of the infiltration velocity between the shoreline and the runup limit are given by KANG and NIELSEN (1994) and KANG (1995).

Irregular, Natural Waves

The situation is more complicated with natural waves because the wind waves themselves are irregular with respect to both period and height, and because groups of wind waves drive surf beats, *i.e.*, oscillations with periods of the order 100s which can be dominant near the shoreline.

Extracting information about the waves' contribution η_w^+ to the total groundwater overheight η^+ (Figure 2) from field data is complicated by the presence of tides. However, the dataset in Figure 3 which contains data from two beaches with identical tides but very different waves offer an opportunity. KANG and NIELSEN (1994) considered the instantaneous differences between those two watertable records and suggested that they could be related to the offshore wave parameters by

$$\eta_{Palm\ Beach} - \eta_{Pittwater} = 0.55 \sqrt{H'_{o,rms} L_o} \tan \beta_F \quad (5)$$

where $H'_{o,rms}$ is the equivalent offshore root mean square wave height, corrected for refraction ($H'_{o,rms} = \sqrt{\cos \alpha_o} H_{o,rms}$ where α_o is the angle between the wave crests and the coast offshore). A more reasonable fit to the data in KANG and NIELSEN's Figure 7 is however

$$\eta_{Palm\ Beach} - \eta_{Pittwater} = 0.1 + 0.44 \sqrt{H'_{o,rms} L_o} \tan \beta_F \quad (6)$$

where the constant 0.1m may be attributed non-linearity, to the difference in tide-generated overheight on the two sides or to a carry-over effect from large waves to subsequent small waves. More data sets are clearly required for a definitive estimator, but in the mean time, we may conclude that the wave generated overheight is of the order

$$\eta_w^+ = 0.44 \sqrt{H'_{o,rms} L_o} \tan \beta_F \quad (7)$$

for steep beaches ($\tan \beta_F > 0.1$) like Palm Beach. This result is analogous to the regular-wave-result (3).

The result (7) which is derived from a set of steep-beach-data should not be uncritically adopted to dissipative conditions where the inner surf zone hydrodynamics are qualitatively different as mentioned above. It is unlikely that η_w^+ should ever be less than the shoreline setup which according to HANSLOW and NIELSEN (1993) is of the order $0.4H_{o,rms}$ or $0.05 \sqrt{H_{o,rms} L_o}$ irrespective of β_F . In fact, the effect of surf beat swash is likely to lift the watertable above the shoreline level on flat beaches so that

$$\eta_w^+ > 0.05 \sqrt{H'_{o,rms} L_o} \quad (8)$$

for all beaches.

TIDAL FORCING

Contrary to the wave effects, the tidal effects on the coastal watertable have been measured directly in the field, *e.g.* the "Pittwater data" in Figure 3 and the dataset of NIELSEN (1990). Also, some modelling success has been achieved using the Dupuit-Forchheimer assumptions and ignoring the cap-

illary fringe, *i.e.*, by considering solutions to the Boussinesq Equation

$$n \frac{\partial h}{\partial t} = K \frac{\partial}{\partial x} \left(h \frac{\partial h}{\partial x} \right) \quad (9)$$

where h is the local height of the watertable above a horizontal, impermeable base, K is the hydraulic conductivity, n is the porosity, x is a shore-normal, horizontal coordinate and t is time.

PHILLIP (1973) showed that a tide of amplitude A_{tide} acting on a vertical beach with undisturbed aquifer depth D , will create an asymptotic overheight compared to the mean sea level (MSL) of

$$\eta_v^+ = \sqrt{D^2 + \frac{1}{2}A_{tide}^2} - D \approx \frac{A_{tide}^2}{4D} \quad (10)$$

and NIELSEN (1990) showed by different means that this height is approached exponentially as

$$\bar{\eta}(c) = \eta_v^+ (1 - e^{-2k_B c}) \quad (11)$$

where k_B is the Boussinesq wave number

$$k_B = \sqrt{\frac{n\omega}{2KD}} \quad (12)$$

NIELSEN (1990) also considered the effect of beach slope and found that an extra overheight is generated if the beach, instead of being vertical, forms the angle β with the horizontal. This overheight is approximately

$$\eta_\beta^+ = 0.5\epsilon A_{tide} \quad (13)$$

a result which is accurate for $\epsilon = k_B A_{tide} / \tan\beta < 0.5$ provided no seepage face is formed. A seepage face formed during the falling tide will cause a further increase of η_β^+ . See the measurements of NIELSEN (1990) and TURNER (1993). For very flat beaches of low permeability η_β^+ will approach the tidal amplitude ($\eta_\beta^+ \rightarrow A_{tide}$), but not exceed it.

THE WIDTH OF THE COASTAL GROUNDWATER ZONE

The width of the coastal strip within which the effects of waves and tides should be included in groundwater models can be estimated by comparing the watertable elevation derived from Dupuit-Forchheimer theory with the sum of overheights created by tides, waves and winds.

For a general scenario as shown in Figure 4 this is the coastal strip within which

$$h_s(x) < D + \eta_v^+ + \eta_\beta^+ + \eta_w^+ + \eta_{wind}^+ \quad (14)$$

The watertable height in an unconfined, shallow aquifer due to the steady recharge rate i and a static ocean level (= MSL) is according to Equation (9) given by

$$h_s(x) = \sqrt{D^2 + \frac{h_r^2 + iL^2/K - D^2}{L}x - \frac{i}{K}x^2} \quad (15)$$

where D is the depth below the MSL of an impermeable boundary and h_r is the watertable height at $x=L$. The overheights due to tides (η_v^+ , η_β^+) and waves (η_w^+) are given by equations (8), (10) and (13) respectively.

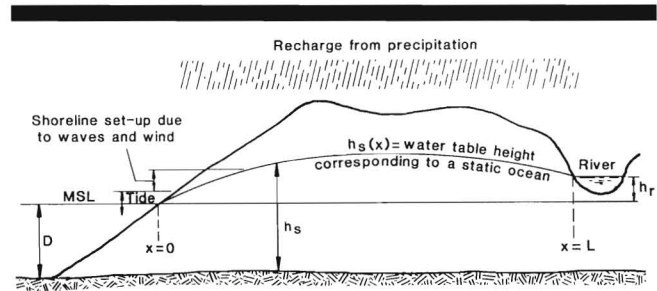


Figure 4. Influence on the watertable height and groundwater salinity from waves and tides can be expected to be significant within a coastal strip where the static-ocean-watertable $h_s(x)$ would be below the highest levels reached by tides and waves.

Under conditions of extreme onshore winds a wind setup may have to be added. The wind setup η_{wind}^+ at the shoreline depends on the wind speed and the wave conditions through the wind stress on the ocean surface. It also depends on the effective length over which the wind acts which may be limited either by the size of the storm or by the width of the continental shelf. No observations of η_{wind}^+ in isolation (with no waves present) are known to the writer but it is clear that η_{wind}^+ may be up to 5 or 6 metres during severe storms on coasts with very wide shelves such as the Gulf Coast of the USA and the N E coast of Australia.

OBSERVED SALINITY STRUCTURE IN A COASTAL BARRIER

The salinity structure under a coastal barrier like the one shown in Figure 1 is quite different from the classical Ghyben-Herzberg case which ignores the input of salt water from wave runup. Without waves, a more or less symmetrical picture is expected with the freshwater flowing out towards both shorelines on top of the salt water and with the local depth $D_L(x)$ of the fresh water lens being of the order

$$D_L(x) = \frac{\rho_{sea}}{\rho_{sea} - \rho_{fresh}} \eta(x) \approx 40\eta(x) \quad (16)$$

in accordance with the Ghyben-Herzberg principle, *cf.* FETTER (1988), pp 150–156. An example of the actual watertable heights and salinity structure measured on Bribie Island North of Brisbane, Australia are shown in Figure 5.

The watertable is seen to be highest near the high water mark and the fresh water lens opens up gradually on the ocean side. It has a maximum thickness of about 1.1m and closes very abruptly on the landward side. A similar scenario was reported by URISH (1980). However, Urish envisaged a more gradual thinning of the freshwater lens on the landward side. Selected salinity profiles are shown in Figure 6.

We note that these profiles are, in general, not showing a sharp interface but a rather gradual increase in salinity with increasing depth below the watertable. The vertical salinity gradients tend to be greatest near the watertable. At the Bribie Island field site, an impermeable layer of “coffee rock” is found between 1.3m and 1.5m below MSL. Below this layer the groundwater is again fresh but rich in hydrogen sulfide.

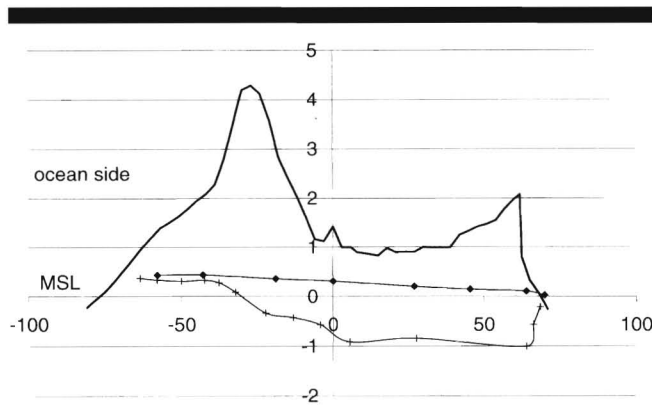


Figure 5. Watertable heights and freshwater displacement thickness measured across the narrow northern part of Bribie Island, 20/7-1997. Measurements in a parallel transect, 100m to the South, have indicated that the situation is practically uniform in the shore parallel direction.

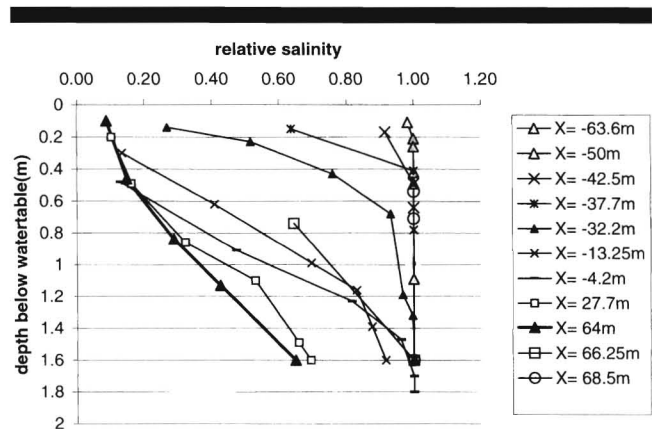


Figure 6. Salinity profiles at selected positions in the Bribie Island transect of Figure 5, 20/7-1997. Note that there is usually not a very sharp interface.

THE MODELLING FRAMEWORK

Modelling of the watertable heights and salinity structure in coastal barriers is attempted in two steps. Firstly, the watertable heights are estimated assuming predominantly horizontal flow. Secondly, the corresponding salinity structure is found in terms of the equivalent local depth $D_L(x,t)$ of the freshwater lens defined as the fresh water displacement thickness

$$D_L = \frac{1}{c_{sea}} \int_{z_{min}}^h (c_{sea} - c) dz \quad (17)$$

where c_{sea} is the salinity of seawater and $c = c(x,z,t)$ is the local instantaneous salinity, *cf.* Figure 7.

The Velocity Potential

In the variable-density groundwater flow, the velocity potential ϕ is a function of z as well as of x and t and it is given by

$$\phi(x, z, t) = K \left[z + \int_z^{h(x,t)} \left(\frac{w}{K} + \frac{\rho}{\rho_{fresh}} \right) dz \right] \quad (18)$$

where w is the vertical flow velocity. In the case of $w \equiv 0$ and uniform freshwater, this potential becomes simply $Kh(x,t)$.

In order to obtain workable, approximate solutions we shall split ϕ into three parts:

$$\phi(x, z, t) = \phi_o(x, t) + \phi_1(x, z, t) + \phi_2(x, z, t) \quad (19)$$

where ϕ_o is the Dupuit-Forchheimer potential

$$\phi_o = Kh(x,t) \quad (20)$$

and ϕ_1 accounts for the approximate density effect based on a sharp interface at $z=h-D_L$, *i.e.*,

$$\phi_1(x, z, t) = \begin{cases} K \int_z^{h-D_L} \left(\frac{\rho}{\rho_{fresh}} - 1 \right) dz & \text{for } z < h - D_L \\ 0 & \text{for } z > h - D_L. \end{cases} \quad (21)$$

If the density is related linearly to the salinity, *e.g.*, as

$$\rho = \rho_{fresh} + \Delta \frac{C}{C_{sea}} = \rho_{fresh} + \frac{\rho_{sea} - \rho_{fresh}}{\rho_{fresh}} \frac{C}{C_{sea}} \quad (22)$$

then the displacement thicknesses based on density and salinity are actually identical and the residual ϕ_2 is zero at $z=0$ as well as at $z=h$, *i.e.*, the picture is qualitatively as in Figure 8.

For purposes of illustration the magnitudes of ϕ_1 and ϕ_2 have been exaggerated by a factor 10 compared with ϕ_o . That is, Figure 8 corresponds to $\Delta=1/4$ instead of the real $\Delta \approx 1/40$

Velocities and Flow Rates

Corresponding to the three components of the velocity potential, the local velocities $u(x,z,t)$ and the depth integrated flow rates $Q(x,t)$ can be written as a sum of the ‘‘Dupuit-Forchheimer contribution’’ which assumes uniform density, a ‘‘sharp interface correction’’ and a residual:

$$\begin{aligned} u(x, z, t) &= u_o(x, t) + u_1(x, z, t) + u_2(x, z, t) \\ &= -K \frac{\partial h}{\partial x} + \begin{cases} K \Delta \frac{\partial D_L}{\partial x} & \text{for } z < h - D_L \\ 0 & \text{for } z > h - D_L \end{cases} \\ &\quad + u_2(x, z, t) \end{aligned} \quad (23)$$

cf. Figure 8. The fact that u_1 is uniform below the assumed interface and zero above makes its flow rate contribution very easy to calculate, we find

$$Q = Q_o + Q_1 + Q_2 = -Kh \frac{\partial h}{\partial x} + K \Delta (h - D_L) \frac{\partial D_L}{\partial x} + Q_2 \quad (24)$$

Due to the fact that the relative density increment $\Delta = (\rho_{sea} - \rho_{fresh})/\rho_{fresh}$ is approximately 1/40, Q_o is usually totally dominant. For the system observed in this study that is the case everywhere except inside the thin diffusive boundary layer where D_L varies much more rapidly than h .

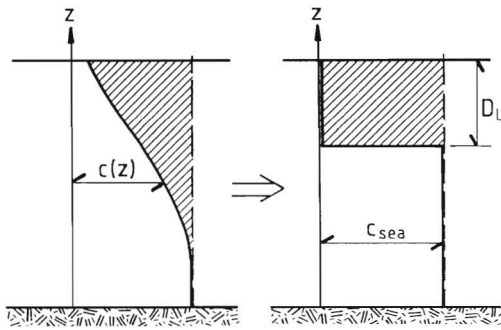


Figure 7. The thickness D_L of the freshwater lens is defined as the fresh-water displacement thickness.

Watertable Heights

If the aquifer is bounded by a horizontal, impermeable layer the watertable height $h(x,t)$ can, in the first instance, be modelled using the 1D equation

$$n \frac{\partial h}{\partial t} = -\frac{\partial Q}{\partial x} + i_s + i_f \tag{25}$$

where, as a first approximation, valid for $h(\partial h/\partial x) \gg \Delta(h - D_L)(\partial D_L/\partial x)$, we can use $Q = Q_o$ leading to the Boussinesq equation

$$n \frac{\partial h}{\partial t} = K \frac{\partial}{\partial x} \left(h \frac{\partial h}{\partial x} \right) + i_s + i_f \tag{9}$$

where $i_s(x,t)$ is the salty recharge rate due to wave runup, occurring only seaward of the runup limit and $i_f(x,t)$ is the fresh water recharge due to rainfall.

The next level of approximation, $Q = Q_o + Q_I$, which ac-

counts approximately for density differences in terms of a sharp interface gives

$$n \frac{\partial h}{\partial t} = K \frac{\partial}{\partial x} \left(h \frac{\partial h}{\partial x} \right) - K \Delta \frac{\partial}{\partial x} \left[(h - D_L) \frac{\partial D_L}{\partial x} \right] + i_s + i_f \tag{26}$$

$$n \frac{\partial h}{\partial t} = K \frac{\partial}{\partial x} \left[\left(h \frac{\partial h}{\partial x} \right) - \Delta (h - D_L) \frac{\partial D_L}{\partial x} \right] + i_s + i_f. \tag{27}$$

The Salinity Structure

In the following we attempt to model the salinity structure with a one dimensional model which describes the behaviour of the thickness $D_L(x,t)$ of the equivalent fresh water lens. The dynamic equation for $D_L(x,t)$ is obtained by expressing the conservation of salt in a control volume of unit length which reads

$$n \frac{\partial}{\partial t} \int_{z=0}^h c \, dz = -\frac{\partial}{\partial x} \int_{z=0}^h cu \, dz - \frac{\partial}{\partial x} \int_{z=0}^h -\epsilon_s \frac{\partial c}{\partial x} \, dz + c_{sea} i_s \tag{28}$$

where the left hand side expresses the rate of change of the local amount of salt and the terms on the right express, respectively, the convective and the diffusive fluxes of salt and the infiltration of salt water. The diffusivity of salt in the x -direction is ϵ_s .

First Approximation: Neglecting Density Differences ($u \equiv u_o$)

Equation (28) is simplified by introducing the freshwater displacement thickness (17). This simplifies the flux terms as indicated in Figure 9 and Equation (28) becomes

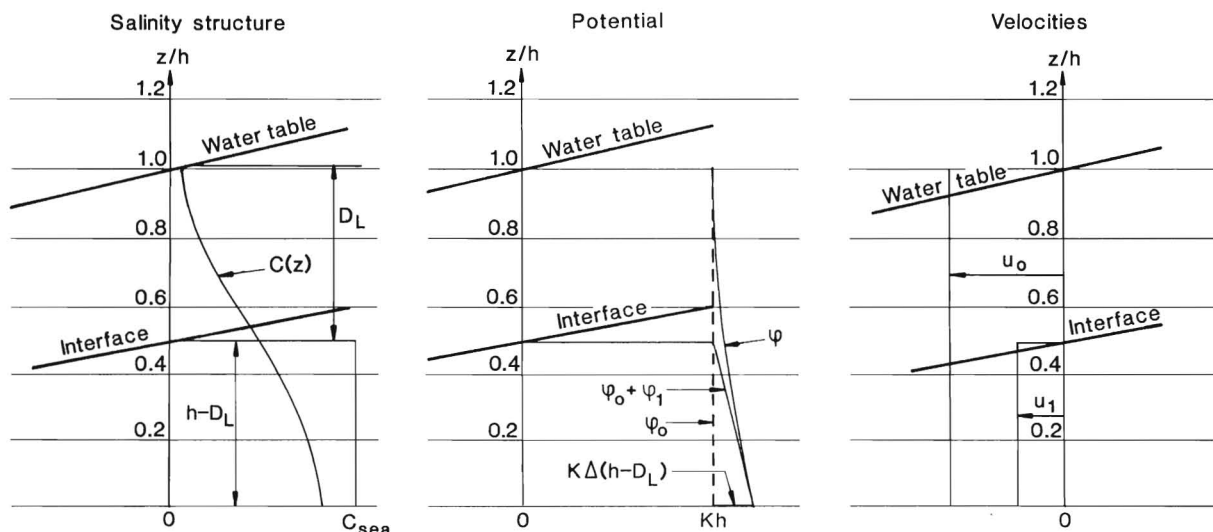


Figure 8. Salinity distribution and the corresponding velocity potential. For illustrative purposes the magnitude of Δ and hence the magnitudes of ϕ_1 and ϕ_2 compared to ϕ_o have been exaggerated by a factor 10.

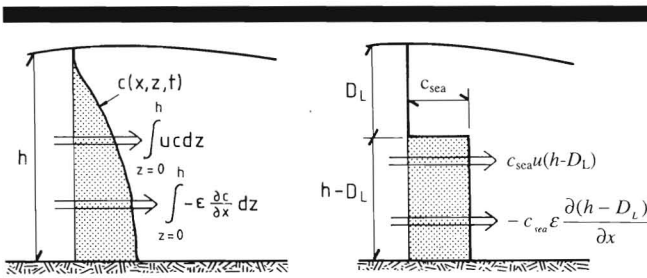


Figure 9. Simplification of the salt flux terms for use in 1D modelling.

$$n \frac{\bar{\sigma}}{\partial t} (c_{sea} [h - D_L]) = - \frac{\bar{\sigma}}{\partial x} (u_o c_{sea} [h - D_L]) - \frac{\bar{\sigma}}{\partial x} \left(-\epsilon_s c_{sea} \frac{\partial [h - D_L]}{\partial x} \right) + c_{sea} i_s \quad (29)$$

which after canceling c_{sea} and with $u_o = -K \partial h / \partial x$ becomes

$$n \frac{\partial (h - D_L)}{\partial t} = K \frac{\partial}{\partial x} \left(h \frac{\partial h}{\partial x} \right) - K \frac{\partial}{\partial x} \left(\frac{\partial h}{\partial x} D_L \right) + \frac{\partial}{\partial x} \left(\epsilon_s \frac{\partial [h - D_L]}{\partial x} \right) + i_s \quad (30)$$

Subtracting this equation from the generalised Boussinesq equation (18) gives

$$n \frac{\partial D_L}{\partial t} = K \frac{\partial}{\partial x} \left(\frac{\partial h}{\partial x} D_L \right) - \frac{\partial}{\partial x} \left(\epsilon_s \frac{\partial [h - D_L]}{\partial x} \right) + i_f \quad (31)$$

This equation is applicable wherever the assumption $u \equiv u_o$ is reasonable, i.e., where

$$\frac{\partial h}{\partial x} \gg \Delta \frac{\partial D_L}{\partial x} \approx \frac{1}{40} \frac{\partial D_L}{\partial x} \quad (32)$$

Accounting for Density Differences Assuming a Sharp Interface

In areas where the freshwater displacement thickness varies more than ten times faster than with x than does h , an extra salt water flux of magnitude Q_1 must be accounted for.

This transforms equation (29) into

$$n \frac{\bar{\sigma}}{\partial t} (c_{sea} [h - D_L]) = - \frac{\bar{\sigma}}{\partial x} [(u_o + u_1) c_{sea} (h - D_L)] - \frac{\bar{\sigma}}{\partial x} \left(-\epsilon_s c_{sea} \frac{\partial [h - D_L]}{\partial x} \right) + c_{sea} i_s \quad (33)$$

where c_{sea} can be cancelled and (the top part of) the expression (23) inserted for $u_o + u_1$. This leads to

$$n \frac{\partial (h - D_L)}{\partial t} = K \frac{\partial}{\partial x} \left[(h - D_L) \left(\frac{\partial h}{\partial x} - \Delta \frac{\partial D_L}{\partial x} \right) \right] + \frac{\partial}{\partial x} \left(\epsilon_s \frac{\partial [h - D_L]}{\partial x} \right) + i_s \quad (34)$$

Subtracting this equation from the corresponding watertable equation (26) leads to

$$n \frac{\partial D_L}{\partial t} = K \frac{\partial}{\partial x} \left(\frac{\partial h}{\partial x} D_L \right) - \frac{\partial}{\partial x} \left(\epsilon_s \frac{\partial [h - D_L]}{\partial x} \right) + i_f \quad (31)$$

same as for the unstratified case. That is, given $h(x,t)$ there is no change to the D_L -equation due to introducing the two layered density structure. This is because (31) is a “fresh-water equation” and the addition of φ_1 , u_1 , and Q_1 adds only a flux of pure salt water under the sharp-interface-assumption, cf Figure 8. However, while the governing equations (9) and (31) for the unstratified problem can be solved separately, the “stratified” system of equations (27)+(31) must be solved simultaneously because of the presence of D_L in (27).

Diffusivity

A diffusion free model may give reasonable predictions of $D_L(x)$ near the ocean side and in the central part. However, it cannot satisfy the boundary condition that the fresh water lens disappears at the right hand boundary. In reality, the lens will disappear gradually due to diffusion of salt throughout the depth. Thus, a complete model requires a reasonable estimate of the diffusivity for salt, ϵ_s .

The longitudinal dispersion coefficient/diffusivity generated by a steady velocity u is according to MARSILY (1986) p 238

$$\epsilon_s = \alpha_L u \quad (35)$$

where α_L is a few centimetres for sand.

Back and forth motion due to tide of the form $u_{tide} = \Delta_{x,tide} \omega \cos \omega t$, where $\omega = 2\pi / T$ is the angular frequency of the tide, can generate further dispersion. The horizontal diffusivity generated by such a motion is, according to Kurzweg and Jaeger (1983) approximately

$$\epsilon_s = 0.075 \Delta_{x,tide}^2 / T = 0.075 \left(\frac{u_{max}}{\omega} \right)^2 \frac{\omega}{2\pi} \quad (36)$$

where $u_{max} = K (\partial h_{tide} / \partial x)_{max}$ and $h_{tide} \approx D + A_{tide} e^{-kx} \cos(\omega t - kx)$ with $k = k_B$, cf Equation (12), this leads to

$$\epsilon_s = 0.012 \frac{n K A_{tide}^2}{D} e^{-2k_B x}$$

Steady State Solutions

Although the natural system will always be changing in response to changing wave conditions and rainfall, it is of interest to consider the shape of the steady state solutions.

NIELSEN (1997) discussed such steady state solutions, simplified by neglecting density differences, at some length. The simplest model which can be used to indicate the general shape of $D_L(x)$ and the thickness of the diffusive boundary layer is

$$D_L(x) = \frac{Q_f(0) + i_f x}{u_o} \left\{ 1 - \exp \left[- \frac{L - x}{\alpha_L + \frac{0.012 n A_{tide}^2 L}{\eta^+ D}} \right] \right\} \quad (37)$$

The factor in front of the bracket describes a steady, diffusion free solution, neglecting density differences and the bracket gives the shape of the diffusive boundary layer under

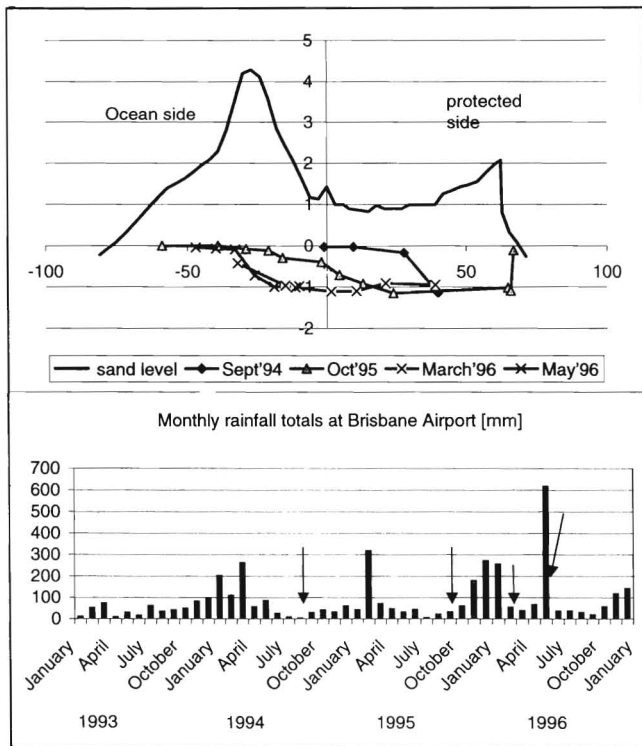


Figure 10. Top, Measured freshwater displacement thickness $D_L(x)$ at different times from the Bribie Island field site plotted downwards from the MSL. Dimensions in metres. Below, Monthly rainfall totals at Brisbane Airport. Arrows point to the times of salinity measurements.

the assumption of constant diffusivity given by (35) and (36) and constant $u_o = -K\eta^+/L$. $Q_f(0)$ is the freshwater flux through the vertical section $x=0$.

This simple approximation shows that the magnitude of the diffusive boundary layer thickness is

$$\delta \approx \alpha_L + 0.012 \frac{nA_{tide}^2 L}{\eta^+ D} \quad (38)$$

which is usually less than two metres.

DYNAMIC CHARACTERISTICS

The wind, wave and rainfall conditions are usually highly variable with large events having the typical duration of two to three days. Therefore, the system will have a considerable dynamic range as indicated by the data in Figure 10.

We see that the measurements following a very dry period in 1994 show almost no freshwater lens under the seaward half of the barrier while the wet weather in May 1996 created a very fat freshwater lens. These measurements are, however, not expected to be the absolute extremes. Larger waves in the period leading up to the 1994 measurements would have driven even more of the freshwater out. Similarly, the first quarter of 1996 was characterised by large waves as well as the high rainfall. That is, if the waves had been smaller, the freshwater lens would have been even thicker and extending further towards the ocean.

The Dynamic Time Scale

The dynamic time scale of the system is of the order $nL^2/(12KD)$ corresponding to the fact that the height of a symmetrical, parabolic watertable above MSL will decay as $\exp\{-t/[nL^2/(12KD)]\}$ after the rain stops. For the system shown in Figure 10 this amounts to 7 days. For initial conditions to be reasonably removed from the numerical results, simulations must be started a few times this time scale before a time of interest.

Residence Time for Pollutants

Water that enters the aquifer a distance L_o from the landward edge of the barrier will take of the order $L_o/(K\eta^+/L)$ to travel to the edge and leave the aquifer. For salt water entering in the runup zone, so that $L_o \approx L$, this residence time is about 520 days for the system shown in Figure 10. Pollutants with the ability to attach themselves to soil particles for longer or shorter periods of time the residence time can be much longer.

DISCUSSION

Due to the infiltration of seawater from wave runup and the asymmetry of tidal in/ex filtration on sloping beaches the groundwater level near the coast (immediately landward of the high water mark) is always considerably above mean sea level. The overheight which depends on beach slope, tidal range and wave conditions may be less than 0.5 during fair weather conditions but it can be several metres during storms. Details of its estimation have been given in sections 3 and 4.

For coastal barriers and ocean atolls which are exposed to waves on one side only, this leads to an asymmetry in the watertable heights and in the shape of the freshwater lens which has consequences for the vegetation and for environmental management. The slope of the watertable drives a steady "landward" groundwater drift which makes the freshwater lens thinner overall and gives it a wedge shape, pointed towards the ocean. On the protected side the freshwater lens ends rather abruptly due to diffusion through a diffusive boundary layer of thickness less than two metres.

The general landward drift of ground water must be considered in relation to wastewater release and management of beach pollution.

The watertable heights, can be modelled without consideration of density variations, *i.e.*, using the generalised Boussinesq equation (9) in areas where D_L varies reasonably slowly (Equation (32)). In areas with very fast variation of the freshwater lens thickness, an extra flux term must be considered, *cf.* Equation (27).

The use of the Boussinesq equation which assumes a shallow aquifer with negligible vertical flow is considered valid in the interior. It is however not appropriate for modelling the details of the infiltration from wave runup. Hence, the infiltration rates that were derived from field and lab experiments by KANG (1995) using the extended Boussinesq equation (9) are to some extent "nominal". It is however consistent and, at this stage, appropriate to use them in connection with (9).

The thickness of the freshwater lens can be modelled satisfactorily using the depth integrated salinity equation developed in Section 7.4. The time dependent equation must be solved numerically, but instructive analytical approximations have been obtained for steady conditions.

Estimates of the diffusivity are provided for both steady flow and oscillatory (tidal) flow. The diffusivity generated by the alternating tidal motion will often dominate within the boundary layer near the protected side.

The time averaged coastal groundwater overheight, quantified in Sections 3 and 4 should be accounted for in regional ground water models through the boundary conditions. That is, such models should use $h = \text{MSL} + \eta'$ at the coastline, not $h = \text{MSL}$.

LITERATURE CITED

- COOPER, H.H., 1959: A hypothesis concerning the balance of fresh water and salt water in a coastal aquifer. *Journal Geophysical Research*, 64(4), 461–467.
- FETTER, C.W., 1988. *Applied Hydrogeology*. Merrill.
- HANSLAW, D.J. and NIELSEN, P., 1993: Shoreline setup on natural beaches. *Journal Coastal Research*, SI No 15, 1–10.
- JAEGER, M.J. and KURZWEIG, U.H., 1983. Determination of the longitudinal dispersion coefficient in flows subjected to high frequency oscillations. *Physics of Fluids*, 26(6), 1380–1382.
- KANG, H-Y., 1995. Watertable Dynamics Forced by Waves. Ph.D. Thesis, Department of Civil Engineering, University of Queensland, 200p.
- KANG, H-Y. and NIELSEN, P., 1994. Watertable overheight due to wave runup on a sandy beach. *Proc 24th Int Conf Coastal Eng (Kobe, A S C E)*, pp. 2115–2124.
- KANG, H-Y.; ASEERVATHAM, A.M., and NIELSEN, P., 1994. Field measurements of wave runup and the beach watertable. *Research Report No CE148*, Department of Civil Engineering, University of Queensland, Brisbane.
- LONGUET-HIGGINS, M.S., 1983. Wave setup, percolation and undertow in the surf zone. *Proceedings Royal Society London*, A390, 283–291.
- MARSILY, G. DE, 1986. *Quantitative Hydrogeology: Groundwater Hydrology for Engineers*. New York: Academic, 440p.
- NIELSEN, P.; DAVIS, G.A.; WINTERBOURNE, J.M., and ELIAS, G., 1988. *Wave Setup and the Watertable in Sandy Beaches*. Tech Memo 88/1, Coast and Rivers Branch, Public Works Dept, Sydney, 132p.
- NIELSEN, P., 1990. Tidal dynamics of the watertable in beaches. *Water Resources Research*, 26(9), 2127–2135.
- NIELSEN, P., 1992. *Coastal Bottom Boundary Layers and Sediment Transport*. Singapore: World Scientific, 324p.
- NIELSEN, P., 1997. Watertable dynamics and salinity in coastal barriers. *Proceedings 13th Australasian Coastal and Ocean Engineering Conference (Christchurch)*, pp. 383–388.
- TURNER, I.L., 1993. Watertable outcropping on macrotidal beaches: A simulation model. *Marine Geology*, 115, 227–238.
- URISH, D.W., 1980. Asymmetric variation of Ghyben Herzberg lens. *Journal Hydraulics Division, Proc A S C E*, 106(HY7), 1149–1158.